Dynamic off-centering of Cr^{3+} ions and short-range magneto-electric clusters in $CdCr_2S_4$

G. N. P. Oliveira,[1,2] A. M. Pereira,[2] A. M. L. Lopes,[1,*] J. S. Amaral,[3] A. M. dos Santos,[4] Y. Ren,[5] T. M. Mendonça,[2] C. T. Sousa,[2] V. S. Amaral,[3] J. G. Correia,[6] and J. P. Araújo[2,†]

[1]*CFNUL-Centro de Física Nuclear, Universidade de Lisboa, Av. Prof. Gama Pinto, 2, 1649-003, Lisboa, Portugal*

[2]*IFIMUP and IN-Institute of Nanoscience and Nanotechnology, Departament of Physics and Astronomy of FCUP, University of Porto, Rua do Campo Alegre, 687, 4169-007 Porto, Portugal*

[3]*CICECO and Department of Physics, Universidade de Aveiro, 3810-193 Aveiro, Portugal*

[4]*Quantum Condensed Matter Division, Oak Ridge National Laboratory, Oak Ridge, Tennessee 37831-6393, USA*

[5]*Advanced Photon Source, Argonne, Argonne National Laboratory, Illinois 60439, USA*

[6]*Instituto Tecnológico e Nuclear, E.N. 10, 2686-953 Sacavém, Portugal*

(Received 24 February 2012; revised manuscript received 10 December 2012; published 26 December 2012)

The cubic spinel $CdCr_2S_4$ gained recently a vivid interest, given the relevance of relaxor-like dielectric behavior in its paramagnetic phase. By a singular combination of local probe techniques, namely, pair distribution function and perturbed angular correlation, we firmly establish that the Cr ion plays the central key role on this exotic phenomenon, namely, through a dynamic off-centering displacement of its coordination sphere. We further show that this off-centering of the magnetic Cr ion gives rise to a peculiar entanglement between the polar and magnetic degrees of freedom, stabilizing, in the paramagnetic phase, short-range magnetic clusters, clearly seen in ultralow-field susceptibility measurements. Moreover, the Landau theory is here used to demonstrate that a linear coupling between the magnetic and polar order parameters is sufficient to justify the appearance of magnetic cluster in the paramagnetic phase of this compound. These results open insights on the hotly debated magnetic and polar interaction, setting a step forward in the reinterpretation of the coupling of different physical degrees of freedom.

DOI: 10.1103/PhysRevB.86.224418 PACS number(s): 77.80.Jk, 64.60.ah, 75.30.Sg, 75.40.Cx

I. INTRODUCTION

Materials with multifunctional physical properties are crucial for the modern society, especially those which display a strong coupling between magnetic and polar degrees of freedom, the so-called multiferroics. This by far unexploited capability promises new paradigm-shift technologies for magnetic data storage, high-frequency magnetic devices, spintronics, and micro-electromechanical systems.[1,2] However, conventional models and theories can not explain the strength of this coupling observed in many examples of multiferroic materials.[3,4] A complete understanding of these macroscopic properties requires a thorough treatment of their atomic-level origins. This coupling is correlated with local distortions, and thus the roles of local polar and magnetic clusters must be determined.[5] Particular interest is currently focused on local distortions in a class of disordered materials, the relaxor-like ferroelectrics, that frequently exhibit a competition/coexistence between short- and long-range orders.[6] $CdCr_2S_4$ is among these relaxor-like systems and is one of the rare compounds that exhibits four colossal effects (the magnetocapacitive, electrocapacitive, electroresistive, and magnetoresistive effects).[7] $CdCr_2S_4$ crystallizes in the spinel structure, with Cd occupying the tetragonal position in the lattice (A site) and Cr^{3+} occupying the octahedral site (B site)[8] [see Fig. 1(a)]. The discovery of dielectric relaxational dynamics above the Curie temperature (T_C), which is responsible for the strongly increased dielectric permittivity of $CdCr_2S_4$, has driven an intense debate in the research community.[9] First-principles calculations exclude softening of the polar modes as a possible origin of the anomalous dielectric behavior.[10] Other models propose that the spin-driven polar moments originate from the off-centering of the Cr^{3+} ions.[9] The $Fd\bar{3}m$ space group of the overall crystal structure forbids the existence of ferroelectric order, but Gnezdilov *et al.* recently suggested a symmetry reduction below T_C from the $Fd\bar{3}m$ to the $F\bar{4}3m$ noncentrosymmetric space group, which permits the existence of electric dipoles. Interestingly, the discovery of phonon anomalies at $T_F < 130$ K suggests that the electronic polarizability is enhanced by the Cr-S distance and respective bond hybridization.[11] Several studies on this topic are available, but the origin of this peculiar dynamic dielectric regime above T_C remains unexplained, and detailed local structural characterization and local probe techniques can provide insights into this phenomenon. Herein, we use pair distribution function (PDF) analysis of x-ray powder diffraction (XRD) data to directly study the local environment of the Cr^{3+} ion. This study is combined with a hyperfine local probe technique, perturbed angular correlation (PAC), which examines the properties and dynamics of the atomic-scale distortions. Spin-lattice correlations are evaluated through low-field magnetization measurements and are phenomenologically described using a modified Landau theory model including a magneto-electric coupling term.

II. EXPERIMENTAL METHODS

The $CdCr_2S_4$ polycrystalline samples studied in this work were synthesized using a solid-state reaction in a double evacuated quartz ampoule.[12–14] The scattering experiments for PDF analysis were performed on beamline 11-ID-C at the Advanced Photon Source at Argonne National Laboratory, over the temperature range 80–220 K. Fourier transforms (Ft) were computed using PDFGETX2, and the fits were performed using PDFFIT2.[15] We used the PDF method to obtain the precise

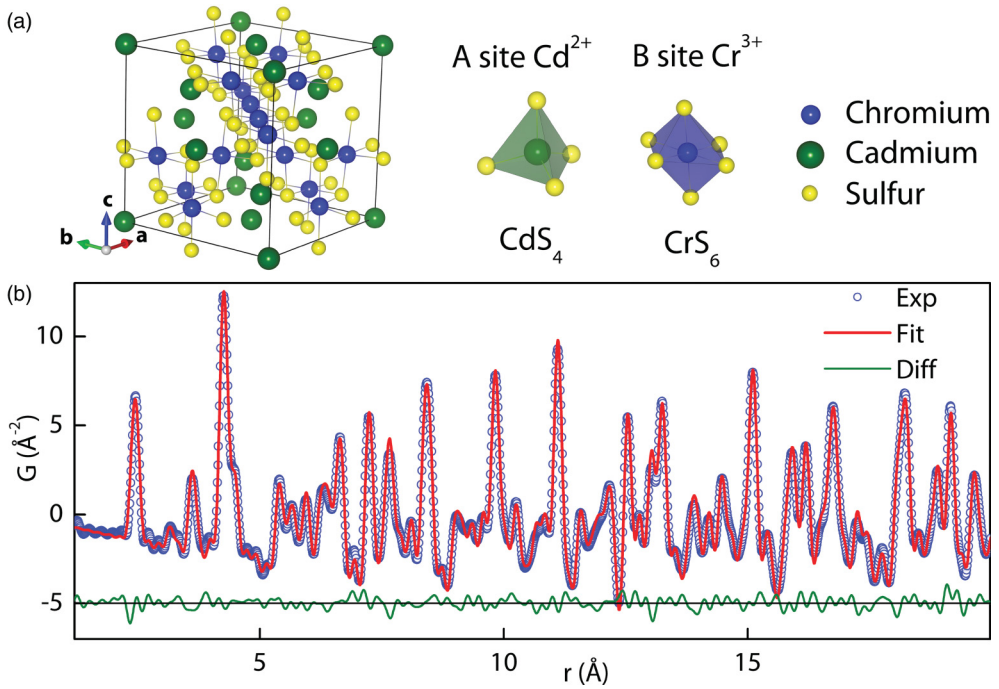

FIG. 1. (Color online) (a) Polyhedron model of the $CdCr_2S_4$ structure. (b) PDF of the spinel $CdCr_2S_4$ structure at 80 K.

structure and size information of atomic structure which is based on the probability of finding pairs of atoms in the material at distance r, given by

$$G(r) = 4\pi r[\rho(r) - \rho_0], \tag{1}$$

where $\rho(r)$ is the atomic-pair density and ρ_0 is the average atomic-number density. $G(r)$ is the scattering-length weight measure of the part obtained via Fourier transform of the reduced total scattering structure function $F(Q)$:

$$G(r) = \frac{2}{\pi}\int_{Q_{\min}}^{\infty} Q[S(Q) - 1]\sin(Qr)dQ, \tag{2}$$

where $S(Q)$ is the structure function obtained after correction and normalization of the diffracted intensity from the sample and Q is the magnitude of the scattering vector. Δr was calculated using the following expression:

$$\Delta r = \sqrt{U_{iso_{\text{expt}}} - U_{iso_{\text{theory}}}}. \tag{3}$$

We used the PAC technique to study the electrical field gradient (EFG) and magnetic hyperfine field (B_{hf}) at an atomic level, specifically at the Cr and Cd sites in this work. The ^{111}In and ^{117}Cd isotopes used were produced in the Isotope Separator On-Line (ISOLDE) CERN Genebra, by ion implantation at 30 keV. To perform the local probe measurements by PAC technique, a six-detector spectrometer (BaF_2) in the temperature range from 300 to 10 K was used. After the implantation, an annealing was performed to the samples in an evacuated quartz ampoule with a sulfur excess. The annealing was performed during 20 min at a temperature of 500 °C (793 K). These annealing conditions have been previously shown to be ideal to allow the system to recover from the implantation damage and keep the sample properties unchanged.[12]

PAC experimental anisotropy function $R(t)$ fit was performed by numerical diagonalization of the interaction Hamiltonian.[16,17] When in the diagonalized form, the EFG principal component V_{zz} and the axial symmetry parameter (η) fully characterize the EFG tensor.[16] In the case of a static electric quadrupole interaction, considering $|V_{zz}| > |V_{yy}| > |V_{xx}|$ and $\eta = (V_{xx} - V_{yy})/V_{zz}$, the perturbation factor for polycrystalline samples can be described as a sum of oscillatory terms and considering the effect of a Lorentzian EFG distribution of relative width δ:

$$G_{kk}(t) = S_{k0} + \sum_n S_{kn}\cos(\omega_n t)e^{-\delta\omega_n t}. \tag{4}$$

The frequencies represented by ω_n are those of the transition frequencies between the hyperfine levels created when a nuclear state is split by the hyperfine interaction. [In the case of ^{111}Cd the intermediate level is characterized by nuclear spin momentum of $I = \frac{5}{2}$. The quadrupole interaction splits this level into three sublevels and thus in the Fts we observe a triplet of frequencies (ω_1, ω_2, $\omega_3 = \omega_1 + \omega_2$) for each nonvanishing EFG distribution present in the system.] For a static interaction, the anisotropy function obtained experimentally can be written as $R(t) = \sum A_{kk}G_{kk}(t)$ where A_{kk} are the angular correlation coefficients of the nuclear decay cascade and G_{kk} contains the perturbation of the angular correlation. In the case of a dynamic electric quadrupole interaction, a different approach is required to characterize the perturbed angular correlation oscillations amplitude. When the characteristic time of the electric field gradient fluctuation is of the same order of magnitude of the PAC time scale, the model of random phase approximation is adopted.[18] In this case, considering the additional term $e^{-\lambda t}$, the perturbation factor for each electric field gradient can be

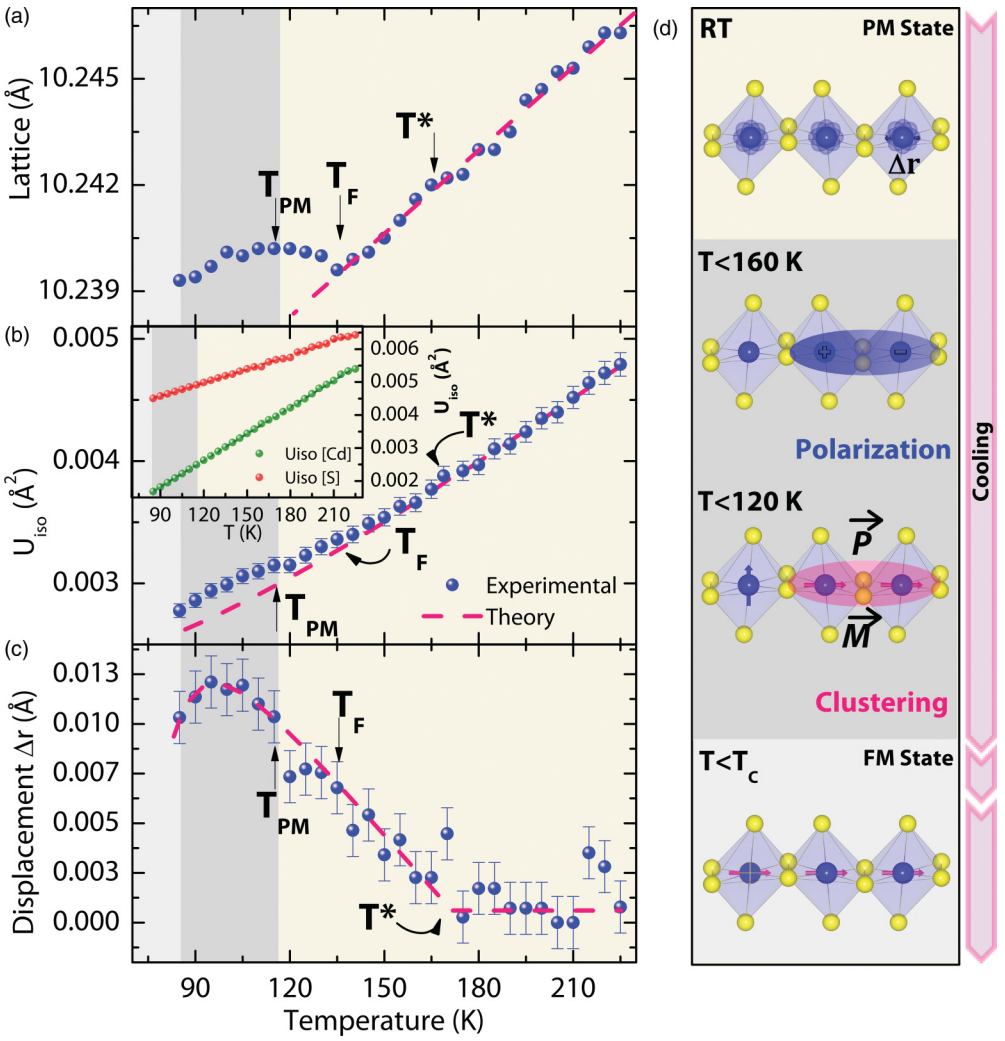

FIG. 2. (Color online) (a) The temperature-dependent lattice parameters. (b) Isotropic ADPs of the Cr atom; inset: isotropic ADPs of the Cd and S atoms. (c) Amplitude of the local Cr off-centering. (d) Schematic representation of the local environment of Cr^{3+} as a function of temperature based on our findings.

described by

$$G_{kk}(t) = e^{-\lambda t}\left(S_{k0} + \sum_n S_{kn}\cos(\omega_n t)e^{-\delta\omega_n t}\right), \qquad (5)$$

where λ is related to the EFG fluctuation rate.[19] Low-field dc magnetization measurements were performed using a commercial magnetometer (MPMS from Quantum Design) over the temperature range 5–370 K in a field-cooling procedure.[20]

III. RESULTS AND DISCUSSION

A representative experimental PDF of $CdCr_2S_4$, collected at 80 K (blue dots), is depicted in Fig. 1(b) along with the corresponding refinement fit beginning with cubic spinel symmetry ($Fd\bar{3}m$) (Ref. 21) (red line) and the residual curve (green). Refinements of similar quality were obtained from the data analyses at different temperatures, and the lattice parameters obtained at room temperature are in agreement with findings from previous reports.[8] The T dependencies of the lattice parameters [$a(T)$] obtained from the Rietveld refinement of the PDFs are depicted in Fig. 2(a). Three distinct regimes were observed over the temperature range 80–220 K. For $T > 130$ K, $a(T)$ exhibits the conventional linear contraction with cooling. This monotonic trend reverses at $T_F \sim 130$ K, where the material begins to exhibit negative thermal expansion, as has been previously observed.[8,22] This negative thermal expansion regime exists within a narrow temperature range, and the negative coefficient of expansion reaches a maximum at $T_{PM} \sim 115$ K before the material returns to the typical thermal contraction regime at lower temperatures. This anomalous thermal behavior is unequivocally indicative of a structural distortion.[23]

In Fig. 2(b), we present the temperature dependence of the isotropic atomic displacement parameter (ADPs [U_{iso}]) of the Cr^{3+} site and Cd and S [inset of Fig. 2(b)], which were refined from the undistorted model. Linear behavior for the Cd and S atoms was observed over the entire temperature range, and no significant deviations from the Einstein model (EM) [dashed lines in Fig. 2(b)] were observed in the ADPs [see inset of Fig. 2(b)], whereas for the Cr atom it is only

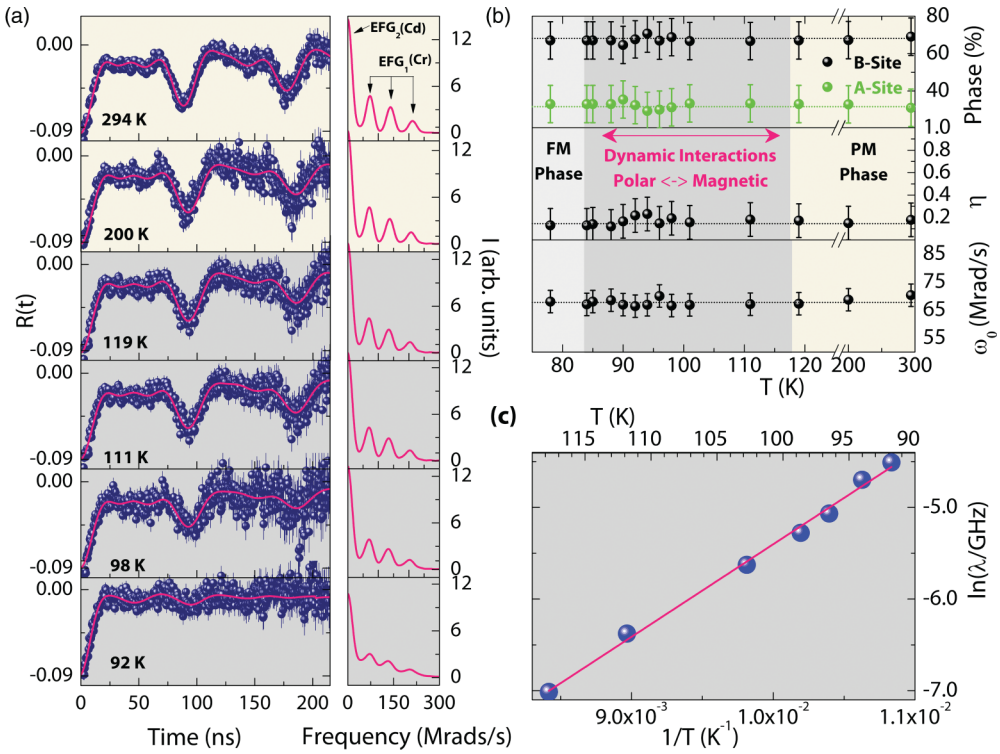

FIG. 3. (Color online) (a) PAC spectra collected at different temperatures. (b) EFG temperature-dependent parameters in the $CdCr_2S_4$ system. (c) PAC dynamic attenuation parameter of the Cr site as a function of the inverse temperature.

observed for $T^* > 160$ K. A deviation from the EM is observed for $T^* < 160$ K and is more pronounced at $T_F = 130$ K. In fact, previous Raman scattering experiments also indicated pronounced anomalies in the intensities and frequencies of optical phonon modes that arose at the same temperature, and these anomalies are consistent with our PDF measurements.[11] This finding is consistent with the appearance of random Cr^{3+} off-center displacements that do not break the cubic symmetry at temperatures below T^*.[23]

The temperature dependence of the amplitude of the Cr off-centering displacements (Δr) is presented in Fig. 2(c), using Eq. (3). A maximum value of 0.012 Å was obtained and is schematically illustrated in Fig. 2(d). The observed displacement amplitude is one order of magnitude lower than that observed in ferroelectric $BaTiO_3$ (Ref. 24) ($\Delta r = 0.24$ Å and $P = \sim 30\ \mu C/cm^2$) and the more recently observed value in chalcogenide compounds (PbTe),[23] where off-centering displacements of Pb^{2+} were observed using the same technique. The displacement obtained here is in good agreement with the lower values of polarization observed for the $CdCr_2S_4$ system ($\Delta r = 0.012$ Å and $P = \sim 0.075\ \mu C/cm^2$).[9]

In order to understand the nature of these displacements at the atomic scale, we performed PAC measurements, which is an excellent tool to probe and study the phenomena present at a microscopic level. The experimental $R(t)$ anisotropy function (blue points on the left) and the respective Ft (red lines on the right) as functions of temperature (294 K > T > 92 K) were obtained using the PAC technique and are depicted in Fig. 3(a). Two coexisting local environments were observed from the ^{111}Cd probes at the Cd (30%) and Cr (70%) sites (^{111}Cd probe is fed by the ^{111}In radioactive decay [^{111}In $\rightarrow$ ^{111} Cd]). These results are consistent with a previous work by *Samokhvalov et al.*[12] where the same probes distribution among the Cd and Cr sites were obtained. The authors justify their results based on the comparison between the theoretical (first-principles calculations) and experimental electric field gradient and magnetic hyperfine field values obtained. Additionally, they show the validity of their findings by combining the results of a set of different isotopes. The set of probes have the same PAC intermediate state, therefore giving a sustained background for this claim. In this way, our fits at $T > 200$ K included two static EFG distributions. EFG_1 is characterized by an observable frequency $\omega_{01} = 68(2)$ Mrad/s [$V_{zz} = 3.6(2) \times 10^{21}$ V/m^2], and an asymmetry parameter $\eta = 0.10(5)$, characteristic of an EFG with a small deviation from axial symmetry as expected for probes at the Cr site.[12] EFG_2 is characterized by an extremely broad frequency distribution with $\omega_{02} \approx 0$ Mrad/s, which is associated with probes at the Cd cubic site. At $T < 200$ K, the $R(t)$ and Ft plots are visibly altered, particularly between 119 and 92 K where $R(t)$ becomes increasingly damped as the temperature decreases. This increased damping of the $R(t)$ spectra is attributed to time-dependent interactions,[25] i.e., EFG fluctuations within the PAC time scale ($1\ \mu s > \tau > 1$ ns; τ is characteristic fluctuation time).[26] This effect can be modeled by including a dynamic attenuation parameter (λ) in the standard static fit function[26] [as introduced in Eq. (5)]. Figure 3(b) presents the fit results at different temperatures; the fraction of each EFG, the asymmetry parameter, and the fundamental frequency are shown at top, middle, and bottom, respectively. Other than the increase of the dynamic attenuation parameter associated with EFG_1 (Cr site), no changes were observed in either EFG. As

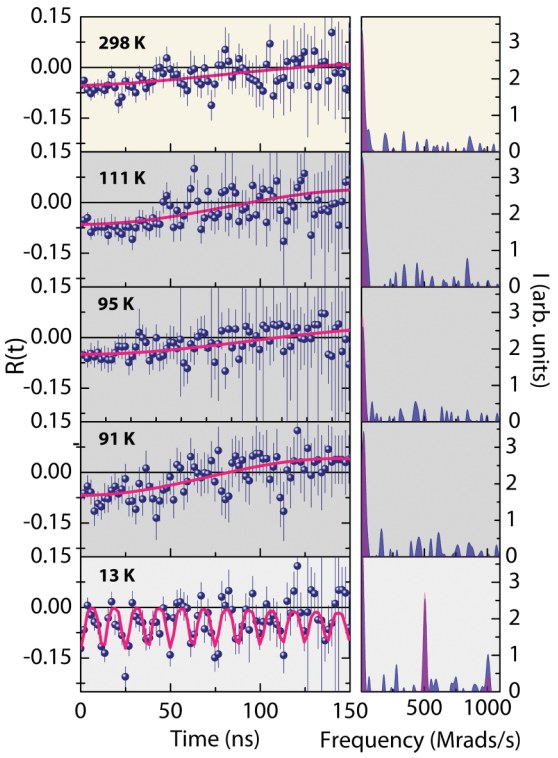

FIG. 4. (Color online) (a) Representative $R(t)$ functions, corresponding fits, and respective Fourier transform taken at different temperatures for the ^{117}Cd probe.

shown in Fig. 3(c), the temperature dependence of the natural logarithm of the dynamic attenuation parameter follows an Arrhenius law with an activation energy of $E_a = 0.1$ eV.[27] The PAC measurements revealed that the Cr site experiences ultraslow dynamics ($\tau > 1$ ns) in the 92–119 K temperature range, while no change was observed in the local environment of the Cd site (the local symmetry remains cubic). These results are in agreement with a model in which the Cr ions hop between equivalent potential energy minima towards an order-disorder-type phase transition[23] occurring below T_C. Additional measurements using the ^{117}Cd→^{117}In probe (^{117}Cd probe replaces only the Cd position) corroborate these results (see Fig. 4).

Figure 4 depicts representative PAC spectra, Fourier transforms, and corresponding fits, obtained from room temperature (RT) to 13 K temperature range for the ^{117}Cd probe in the $CdCr_2S_4$ system. Our results (in accordance with the previous one[12]) in the 91 K to RT temperature range, paramagnetic state, show only a time-independent EFG, characteristic of an A-site substitution. Knowing the A site has local cubic environment, then a null EFG should be expected. However, experimentally it is common to observe instead a large distribution around zero, like in the present case. Note that, in all temperature ranges, no changes are observed in the $R(t)$ spectra. Whereas an "exponential" damping of the $R(t)$ function would be expected if a dynamic interaction was present in a certain range of temperatures. In the ferromagnetic state, as expected,[12] the presence of a single magnetic interaction having a high Larmor frequency is observed. Thus, the absence of changes in the $R(t)$ spectra above T_C points for the fact that no dynamic distortions occur around the Cd site. Therefore, the dynamics distortions observed in the previous results (using the ^{111}In probe) can be exclusively attributed to the B site.

The combined analysis of the PDF and PAC results indicates that the dynamic Cr^{3+} off-center displacements occur well above T_C ($T < T^*$). Furthermore, the average size of the randomly oriented dipoles (formed by the off-centering of the Cr ions) increases as the temperature decreases and saturates at T_{PM} [see Fig. 1(d)]. The correlated onset of a critical dynamic slowing of these entities is also observed at approximately T_{PM}. These ultraslow dynamics exhibit the signatures of a phase transition with order-disorder features and eventually result in the recently reported $Fd\bar{3}m$ to noncentrosymmetric $F\bar{4}3m$ phase transition.[11] In fact, a recent LSDA + U calculation suggests that the origin of the observed relaxor behavior in $CdCr_2S_4$ is distinct from a displacive polar soft mode,[10] which was experimentally verified using far-infrared analysis.[28]

Because the Cr^{3+} ions are magnetic ions, displacements of these atoms should produce macroscopic anomalies in the magnetization properties. In fact, in the very low-field measurements ($H < 103$ Oe), we observed a steplike behavior in the temperature dependence of the reciprocal susceptibility ($\chi^{-1} = H/M$) that has not yet been reported [depicted in Fig. 5(a)]. This step occurs in the temperature range between the ordering temperature $T_C \sim 86$ K and $T_{PM} \sim 116$ K. This feature in the paramagnetic (PM) regime indicates the presence of short-range magnetic clusters (SRMC).[20] As H increases, $\chi^{-1}(T)$ tends to have only one plateau [see Fig. 5(a)], and the magnetic susceptibility data at $H \geqslant 100$ Oe show a trend nearly identical to that of the high-temperature data. Nevertheless, we highlight that even at $T \gg T_C$ and $H > 100$ Oe, some small curvature in χ^{-1} is still observable, which indicates that a cooperative short-range process is still present up to $T^* \sim 160$ K [see inset in Fig. 5(a)]. These observations are in agreement with the PDF results, which indicate that the Cr atomic displacement seemingly persists up to T^*. Above this temperature, $\chi^{-1}(T)$ enters a nearly linear regime, and an effective paramagnetic moment of $\mu_{\text{eff}} = 4.15\ \mu_B$/Cr can be determined [see inset in Fig. 5(a)]. This value is higher than the expected value of $3.87\mu_B/Cr^{3+}$(half-filled lower t_{2g} triplet with a spin $S = \frac{3}{2}$ and $g = 1.984$, as measured by Berzhansky *et al.*[29]), demonstrating the presence of short-range magnetic correlations even at higher temperatures.

The observed SRMC are dependent on the magnetic field, which results in different $\chi^{-1}(T)$ slopes that correspond to different magnetic cluster sizes.[20] Applying a Curie-Weiss law in the $T_C < T < T_{PM}$ region, a $\mu_{\text{eff}} = 4.1\mu_B$/Cr for $H = 103$ Oe and $9.4\mu_B$/Cr for $H = 1$ Oe were obtained. This result demonstrates that only a small number of ions are involved in the SRMC, which is in agreement with the correlation length of 5.3 Å obtained from the PDF data (at $T = 100$ K, where the Cr off-centering has its maximum). This result was obtained by using the method described by Qiu *et al.* considering the Cr-Cr(Cd, S) bond lengths.[30] This magnetic effect overcomes the mysterious behavior previously observed using ESR, for which a polaronlike mechanism was suggested.[31] The atomic displacements of the Cr^{3+} ions lead to correlated polar and magnetic effects in the paramagnetic/electric regime and indicate the presence of a polar-magnetic coupling. Comparing the effect of a magnetic field unveiled by our results and

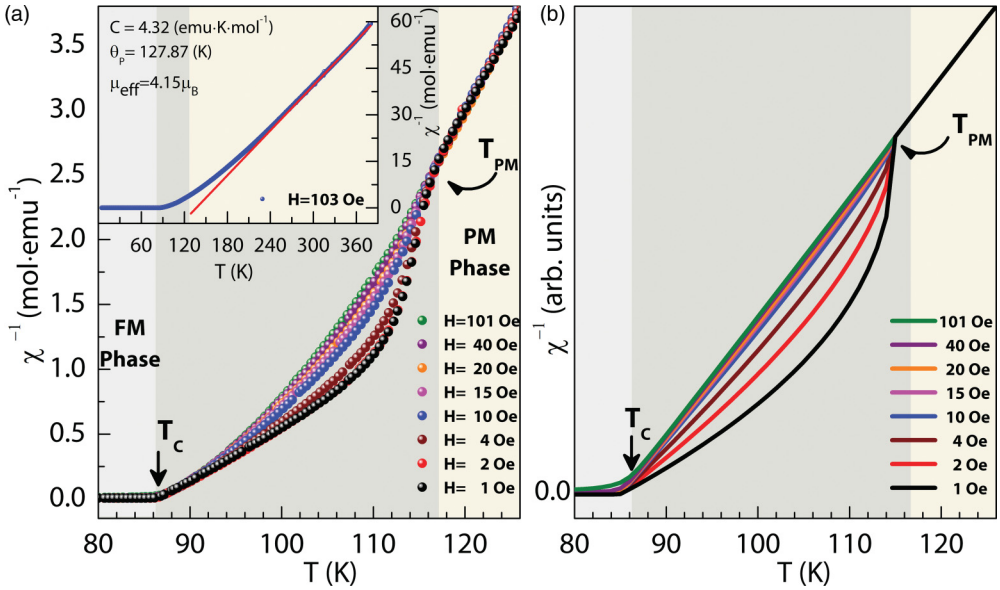

FIG. 5. (Color online) (a) $\chi^{-1}(T)$ at different applied magnetic fields 1–101 Oe. Inset: $\chi^{-1}(T)$ measured upon heating and with $H =$ 103 Oe. (b) $\chi^{-1}(T)$ resulting from theoretical calculations of the phase transitions using the Landau theory, considering a linear magneto-electric coupling.

those in Ref. 9 [Fig. 2(b)], one observes that the magnetic and dielectric responses seem to oppose each other, i.e., whereas magnetic clustering decreases with the magnetic field, the low-frequency dielectric response is enhanced by it.[9] This result suggests that the Cr ions in a cluster tend to displace towards each other to enhance their coupling at low fields, while larger fields cause the ions to become displaced in a uniform direction, producing an increased dielectric constant.

In a typical Landau theory free-energy expansion (G) in powers of magnetization (M) and polarization (P), including magneto-electric coupling terms (αPM) up to the second order (spin-lattice coupling) and ferroic behavior for both order parameters, G is given by

$$G = \tfrac{1}{2}A\,(T - T_C)\,M^2 + \tfrac{1}{4}BM^4 + \tfrac{1}{2}A'\,(T - T_{PM})\,P^2 + \tfrac{1}{4}B'P^4 - MH - PE - \alpha PM, \quad (6)$$

where A, B, A', B', and α are constants, E is the electric field, T_C is the macroscopic ferromagnetic ordering temperature (86 K), and T_{PM} is the temperature value at which the multiferroic clusters emerge, i.e., the Cr ion distortion is close to its maximum. An immediate conclusion from this formulation [Eq. (6)] is that a nonzero magnetization value for $T_C < T < T_{PM}$ can emerge as a consequence of magneto-electric coupling. The order of the coupling term will affect the general properties of these dependencies, which will be visible in the $\chi^{-1}(T)$ plots when only the terms with a linear dependency on M are considered. Behavior similar to that of the experimental $\chi^{-1}(T)$ is reproduced [see Fig. 5(b)] when simulating with the applied magnetic field values (and $E = 0$). Numerical values for the A and B coefficients were obtained by fitting the Arrott plots of the magnetization data for $H > 1$ kOe. The A' and B' coefficients were chosen to produce $\sim 10\mu$ C/cm^2 values of P, as an estimate of the local polarization.[9] The resulting value of the linear magneto-electric coefficient is then $\alpha \sim 1 \times 10^{-2}$ mV/(cm Oe), which is within the typical range of single-phase multiferroics.[3] These findings provide evidence for a scenario in which a magneto-electric coupling is present (magnetization↔polarization) and the magnetic and electric anomalies arise from the Cr^{3+} displacement, in accord with our findings. Note that these abnormal reciprocal susceptibility features have also been observed in other compounds that present strong interplay between the lattice and spin degrees of freedom (R_5[Si,Ge]$_4$ and La[Sr,Ca]MO);[20,32–34] thus, a similar analysis may explain these observations.

IV. CONCLUSIONS

In summary, our experimental PDF, PAC, and $M(T)$ results demonstrate the existence of a dynamic state caused by the presence of simultaneous polar and magnetic nanoclusters, indicating that the system exhibits a birelaxor nature. Our results are consistent with a model in which the effects described in the recent literature arise from atomic displacements of Cr^{3+} ions occurring well above the magnetic ordering temperature. Our combined analysis clearly reveals that the increase in the average size of randomly oriented dipoles saturates at T_{PM}, concomitantly with the onsets of their dynamic slowing and the Cr^{3+}-Cr^{3+} magnetic correlations. Finally, we further demonstrate that an ultraslow Cr^{3+} displacement dynamics precedes the recently reported $Fd\bar{3}m$ to noncentrosymmetric $F\bar{4}3m$ phase transition, suggesting its order-disorder-type origin. This Cr^{3+} dynamic off-centering is intrinsically entangled with the formation of local dipoles and is also responsible for the observed magnetic correlations between adjacent Cr^{3+} neighbors. We further confirm this coupling of electric and magnetic orders by modeling the peculiar low-field $\chi^{-1}(T)$ measurements using Landau theory with a linear magneto-electric term. We believe that this is a step

forward in understanding the exotic behavior of (bi)relaxor systems and their entanglement with lattice distortions.

ACKNOWLEDGMENTS

The authors gratefully thank the ISOLDE Collaboration for the assistance with PAC measurements, and a special thanks to V. Tsurkan for the discussions. This work was supported by FCT-Portugal with projects PTDC/FIS/105416/2008, CERN/FP/109357/2009, and CERN/FP/116320/2010; FEDER/POCTI/n2-155/94 and the ISOLDE collaboration with approved project IS487, and the European Union: FP6 RII3-EURONS, Contract No. 506065 and FP7-through ENSAR, Contract No. 262010. Use of the Advanced Photon Source at Argonne National Laboratory was supported by the US Department of Energy, Office of Science, Office of Basic Energy Sciences, under Contract No. DE-AC02- 06CH11357. AMdS acknowledges the support of the Scientific User Facilities Division, Office of Basic Energy Sciences, U.S. Department of Energy. G.N.P.O. (Grant No. SFRH/BD/80112/2011), A.M.P. (Grant No. SFRH/BPD/63150/2009), C.T.S., T.M.M., and J.S.A. (Grant No. SFRH/BPD/63942/2009) are thankful for their FCT Grants.

*armandina.lima.lopes@cern.ch
†jearaujo@fc.up.pt

[1] T. Kimura, T. Goto, H. Shintani, K. Ishizaka, T. Arima, and Y. Tokura, Nature (London) **426**, 55 (2003).
[2] T. Goto, T. Kimura, G. Lawes, A. P. Ramirez, and Y. Tokura, Phys. Rev. Lett. **92**, 257201 (2004).
[3] W. Eerenstein, N. D. Mathur, and J. F. Scott, Nature (London) **442**, 759 (2006).
[4] Y.-H. Chu, L. W. Martin, M. B. Holcomb, M. Gajek, S.-J. Han, Q. He, N. Balke, C.-H. Yang, D. Lee, W. Hu, Q. Zhan, P.-L. Yang, A. Fraile-Rodriguez, A. Scholl, S. X. Wang, and R. Ramesh, Nat. Mater. **7**, 478 (2008); **7**, 678 (2008).
[5] A. M. L. Lopes, J. P. Araújo, V. S. Amaral, J. G. Correia, Y. Tomioka, and Y. Tokura, Phys. Rev. Lett. **100**, 155702 (2008).
[6] G. Y. Xu, J. S. Wen, C. Stock, and P. M. Gehring, Nat. Mater. **7**, 562 (2008).
[7] C. P. Sun, C. L. Huang, C. C. Lin, J. L. Her, C. J. Ho, J. Y. Lin, H. Berger, and H. D. Yang, Appl. Phys. Lett. **96**, 122109 (2010).
[8] P. K. Baltzer, H. W. Lehmann, and M. Robbins, Phys. Rev. Lett. **15**, 493 (1965).
[9] J. Hemberger, P. Lunkenheimer, R. Fichtl, H. A. K. von Nidda, V. Tsurkan, and A. Loidl, Nature (London) **434**, 364 (2005); **448**, E5 (2007).
[10] C. J. Fennie and K. M. Rabe, Phys. Rev. B **72**, 214123 (2005).
[11] V. Gnezdilov, P. Lemmens, Y. G. Pashkevich, C. Payen, K. Y. Choi, J. Hemberger, A. Loidl, and V. Tsurkan, Phys. Rev. B **84**, 045106 (2011).
[12] V. Samokhvalov, S. Unterricker, I. Burlakova, F. Schneider, A. Dietrich, V. Tsurkan, I. M. Tiginyanu, and I. Collaboration, J. Phys. Chem. Solids **64**, 2069 (2003).
[13] R. A. W. Haul and F. R. L. Schöning, Z. Anorg. Allg. Chem. **269**, 120 (1952).
[14] V. Tsurkan (private communication).
[15] C. L. Farrow, P. Juhas, J. W. Liu, D. Bryndin, E. S. Bozin, J. Bloch, T. Proffen, and S. J. L. Billinge, J. Phys.: Condens. Matter **19**, 335219 (2007).
[16] G. Schatz and A. Weidinger, *Nuclear Condensed Matter Physics: Nuclear Methods and Applications* (Wiley, Chichester, 1996).
[17] A. M. L. Lopes, J. P. Araújo, J. J. Ramasco, V. S. Amaral, R. Suryanarayanan, and J. G. Correia, Phys. Rev. B **73**, 100408(R) (2006).
[18] D. Bohm and D. Pines, Phys. Rev. **92**, 609 (1953).
[19] H. Winkler and E. Gerdau, Z. Phys. **262**, 363 (1973).
[20] C. Magen, P. A. Algarabel, L. Morellon, J. P. Araújo, C. Ritter, M. R. Ibarra, A. M. Pereira, and J. B. Sousa, Phys. Rev. Lett. **96**, 167201 (2006).
[21] T. N. Borovskaya, L. A. Butman, V. G. Tsirelson, M. A. Poraikoshits, T. G. Aminov, and R. P. Ozerov, Kristallografiya **36**, 612 (1991).
[22] F. Bridges, L. Downward, Y. Jiang, and I. O'Brien, EXAFS **882**, 59 (2007).
[23] E. S. Bözin, C. D. Malliakas, P. Souvatzis, T. Proffen, N. A. Spaldin, M. G. Kanatzidis, and S. J. L. Billinge, Science **330**, 1660 (2010).
[24] G. H. Kwei, A. C. Lawson, S. J. L. Billinge, and S. W. Cheong, J. Phys. Chem. **97**, 2368 (1993).
[25] S. N. Mishra, M. Rots, and S. Cottenier, J. Phys.: Condens. Matter **22**, 385602 (2010).
[26] A. Baudry and P. Boyer, Hyperfine Interact. **35**, 803 (1987).
[27] A. Lahmar, S. Habouti, C. H. Solterbeck, M. Es-Souni, and B. Elouadi, J. Appl. Phys. **105**, 014111 (2009).
[28] T. Rudolf, C. Kant, F. Mayr, J. Hemberger, V. Tsurkan, and A. Loidl, Phys. Rev. B **76**, 174307 (2007).
[29] V. N. Berzhansky, V. I. Ivanov, and A. V. Lazuta, Solid State Commun. **44**, 771 (1982).
[30] X. Qiu, T. Proffen, J. F. Mitchell, and S. J. L. Billinge, Phys. Rev. Lett. **94**, 177203 (2005).
[31] Z. Yang, X. Bao, S. Tan, and Y. Zhang, Phys. Rev. B **69**, 144407 (2004).
[32] V. S. Amaral, J. P. Araújo, Y. G. Pogorelov, J. B. Sousa, P. B. Tavares, J. M. Vieira, J. M. B. L. dos Santos, A. A. C. S. Lourenco, and P. A. Algarabel, J. Appl. Phys. **83**, 7154 (1998).
[33] W. J. Jiang, X. Z. Zhou, G. Williams, Y. Mukovskii, and R. Privezentsev, J. Phys.: Condens. Matter **21**, 415603 (2009).
[34] A. M. Pereira, L. Morellon, C. Magen, J. Ventura, P. A. Algarabel, M. R. Ibarra, J. B. Sousa, and J. P. Araújo, Phys. Rev. B **82**, 172406 (2010).